Transmission-line resonators for the study of individual two-level tunneling systems

Jan David Brehm, Alexander Bilmes, Georg Weiss, Alexey V. Ustinov, and Jürgen Lisenfeld

Citation: Appl. Phys. Lett. **111**, 112601 (2017);
View online: https://doi.org/10.1063/1.5001920
View Table of Contents: http://aip.scitation.org/toc/apl/111/11
Published by the American Institute of Physics

Transmission-line resonators for the study of individual two-level tunneling systems

Jan David Brehm,[1] Alexander Bilmes,[1] Georg Weiss,[1] Alexey V. Ustinov,[1,2] and Jürgen Lisenfeld[1]
[1]*Physikalisches Institut, Karlsruhe Institute of Technology, 76131 Karlsruhe, Germany*
[2]*Russian Quantum Center, National University of Science and Technology MISIS, Moscow 119049, Russia*

(Received 19 April 2017; accepted 28 August 2017; published online 12 September 2017)

Parasitic two-level tunneling systems (TLS) emerge in amorphous dielectrics and constitute a serious nuisance for various microfabricated devices, where they act as a source of noise and decoherence. Here, we demonstrate a new test bed for the study of TLS in various materials which provides access to properties of individual TLS as well as their ensemble response. We terminate a superconducting transmission-line resonator with a capacitor that hosts TLS in its dielectric. By tuning TLS via applied mechanical strain, we observe the signatures of individual TLS strongly coupled to the resonator in its transmission characteristics and extract the coupling components of their dipole moments and energy relaxation rates. The strong and well-defined coupling to the TLS bath results in pronounced resonator frequency fluctuations and excess phase noise, through which we can study TLS ensemble effects such as spectral diffusion, and probe theoretical models of TLS interactions.
[http://dx.doi.org/10.1063/1.5001920]

With the advent of experimental techniques to observe and manipulate the quantum states of superconducting circuits such as quantum bits and microwave resonators, two-level tunnelling systems (TLS) have been rediscovered as a major source of noise and decoherence. TLS are believed to originate from the tunnelling of an atomic entity between two nearby positions in a disordered material, giving rise to microscopic elastic and, if charged, electric dipoles which couple to electric fields and mechanical strain.[1,2] In recent years, TLS which reside in amorphous dielectrics such as surface oxides or insulating coatings were increasingly recognized as important performance-limiting culprits in various systems, ranging from micromechanical resonators (MEMSs) through kinetic inductance photon detectors (MKIDs) to interferometer mirrors used in gravitational wave detection.[3–5] After it was recognized that TLS within the tunnel barrier of a Josephson junction were the origin of avoided level crossings observed in spectroscopy of a superconducting phase qubit,[6] this type of device was utilized to achieve quantum state control and readout of individual TLS.[7,8] In such experiments, the ability to tune TLS via an applied mechanical strain[9] has proven to be particularly useful for studying TLS interactions[10] and decoherence.[11,12]

Employing qubits to study TLS is so far limited to addressing TLS in tunnel junction barriers, which for technical reasons are almost exclusively fabricated from thin (≈2 nm) layers of amorphous aluminum oxide, precluding studies on TLS in different materials. Only recently, strong coupling to individual TLS was observed using a superconducting lumped element LC-resonator which featured electric field tuning of TLS.[13] Here, we present an alternative approach of addressing single TLS: We terminate a $\lambda/2$ transmission line resonator with an overlap capacitor that hosts TLS in its dielectric, and we tune TLS by mechanical strain rather than by an electric field. This setup constitutes a circuit-QED system with the dynamics described by the Jaynes-Cummings model,[14] in which the coupling strength between a TLS and the resonator is given by $g = (\Delta/E)\ p_{\parallel}\ |E_{\mathrm{RMS}}|$, where $p_{\parallel}$ is the component of the TLS' dipole moment that is parallel to the oscillating electric field of amplitude $|E_{\mathrm{RMS}}|$ in the capacitor, E is the TLS' excitation energy, and Δ is the tunneling energy between states. The coupling gives rise to a hybridization of TLS with cavity states and lifts the degeneracy of the corresponding excitation manifold. Depending on the TLS-resonator detuning δ, the system shows either a resonant behavior or state-dependent dispersive resonance shifts by $2g^2/\delta$ for large detuning ($\delta > g$).[14]

A sketch of our experimental setup and a sample photograph are shown in Fig. 1(a). The resonators are optically patterned from an Al film to form coplanar transmission lines of length $\lambda/2$ at a desired resonance frequency range from 5 to 6 GHz. One end of the resonator's center strip is designed to overlap with a segment of the Al ground plane onto which AlO_x has been deposited, thus forming an Al/AlO_x/Al plate capacitor as shown in the magnified inset to Fig. 1(a) and sketched in Fig. 1(b). The amorphous AlO_x is fabricated using anodic oxidation of the ground plane to a desired thickness of $t = 50$ nm. To vary the dielectric volume $V_{\mathrm{diel}} = 10\,\mu\mathrm{m}\cdot t\cdot s$ in the capacitor, we modify the overlap length s, resulting in the parameters summarized in Table I for the three tested resonators.

For readout, the other end of the resonator is capacitively coupled to a transmission line whose input part is heavily attenuated and filtered at low temperatures. The output signal passes through two isolators and a large-gain, low-noise HEMT amplifier at 4.2 K and two additional amplifiers at room temperature. The transmission S_{21} is recorded as a function of frequency using a network analyzer, see Fig. 2(b) for a

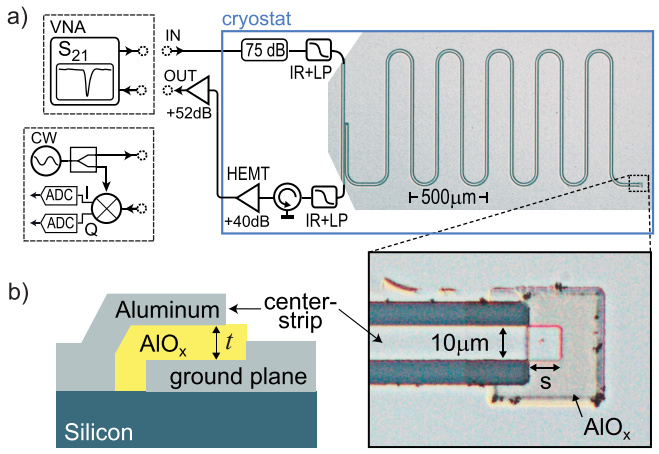

FIG. 1. (a) Schematic of the experimental setup and photograph of a sample, which is a $\frac{\lambda}{2}$-resonator terminated by an Al/AlO_x/Al capacitor as shown in the inset magnification. The dielectric volume of the capacitor is $10\,\mu m \cdot s \cdot t$, with the AlO_x-thickness of $t = 50$ nm and lengths of $s = \{5, 10, \text{and } 15\}$ μm. The other end is capacitively coupled to a transmission line equipped with infrared (IR) and low-pass (LP) filters, isolators, a HEMT-amplifier at 4.2 K, and additional room-temperature amplifiers. Measurements are done using either a network analyzer (VNA) or a continuous-wave (CW) microwave source and an IQ-mixer, whose I and Q outputs are sampled using fast analog to digital converters (ADC). (b) Sketch of a capacitor cross-section.

typical result. The mechanical strain is controlled via the voltage V_p applied to a piezo actuator which slightly bends the sample chip as described in Ref. 9, resulting in a strain field $\epsilon \approx (8 \times 10^{-7}/\text{V}) \cdot V_p$. All data in this work were acquired at a sample temperature of 35 mK.

TLS spectroscopy is performed by recording the resonator transmission S_{21} as a function of the applied mechanical strain. The excitation energy of a TLS is given by $E = \sqrt{\Delta^2 + \varepsilon^2}$, where Δ is the (constant) tunnelling energy between the states and $\varepsilon = 2\gamma(\epsilon - \epsilon_0)$ is the asymmetry energy which scales with the TLS' deformation potential γ and the effective strain field ϵ.[15] This hyperbolic dependence of TLS resonance frequencies can be directly observed by changes in the resonator transmission if the system is driven at powers below the one-photon-regime. In this power range, TLS saturation effects can be neglected.[15] We note that all here observed TLS signatures are in the direct vicinity of the TLS' symmetry points ($\varepsilon < 10$ MHz) such that $\Delta/E \approx 1$ is valid in good approximation.

Figure 2(a) gives an example of such a measurement, plotting S_{21} as a function of the applied piezo voltage. In the shown strain range, we observed about ten hyperbolic TLS traces, whose origins are marked by arrows. Fits to these traces directly result in the static TLS parameters Δ and γ. For the deformation potentials γ, we find values ranging between 0.1 and 1 eV (see also supplementary material), which are consistent with TLS ensemble measurements obtained on bulk AlO_x[11] and with experiments on individual TLS in tunnel junction barriers.[9] From extended measurements over a wider strain range, one could hypothetically reconstruct the distribution of tunnelling energies Δ in order to verify a central assumption of the standard TLS model.[2,15] By counting the number of visible hyperbolas, we extract densities of strongly

TABLE I. Parameters of three tested resonators. s is the designed lateral capacitor size (see Fig. 1), C its capacitance, and V_{diel} the corresponding volume of its AlO_x dielectric. f_{res} is the measured resonance frequency. The values of the coupling quality factor Q_c, the unsaturated loss tangent $F\tan(\delta_0)$, the critical power P_c, and the exponent β are extracted from fits to the power-dependent resonator loss rate Eq. (1). The errors on P_c are smaller than 10^{-3} dBm and therefore not shown.

#	s (μm)	V_{diel} (μm^3)	C (fF)	f_{res} (GHz)	Q_c (10^4)	$F\tan(\delta_0)$ (10^{-4})	P_c (dBm)	β
1	5	2.5	89	5.15775	29.3	0.4 ± 0.1	–145	0.97 ± 0.12
2	10	5.0	178	5.46320	28.8	2.2 ± 0.2	–145.6	1.19 ± 0.03
3	20	10	356	5.58385	22.7	1.9 ± 0.3	–142.7	1.23 ± 0.06

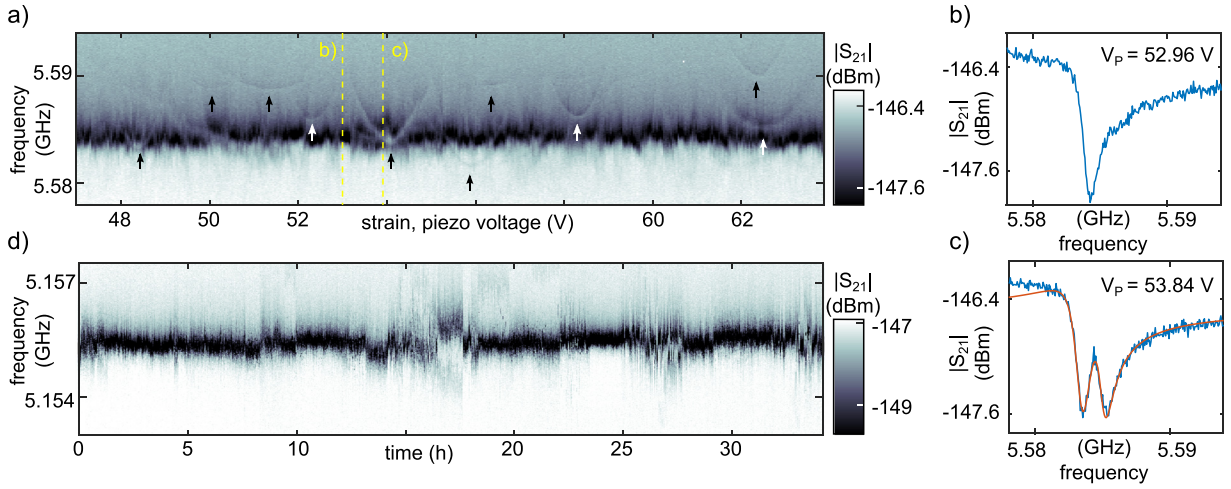

FIG. 2. (a) Transmission $|S_{21}|$ (color-coded) of resonator 3 vs. frequency (vertical axis) and mechanical strain (in units of the applied piezo voltage, horizontal axis). Interaction with strongly coupled TLS is observed by hyperbolic traces when their resonance frequencies are strain-tuned through their symmetry points (indicated by arrows). Vertical dashed lines correspond to the cross-sections shown in (b) and (c). (b) Typical resonator transmission vs. frequency. (c) The transmission amplitude shows a double-dip feature due to a strongly coupled TLS near resonance with the resonator. The solid red line is a fit to the theory, resulting in the TLS' decoherence rate, coupling strength, and gap energy. (d) Transmission of resonator 1 as a function of time at constant mechanical strain. Spectral TLS diffusion is observed by pronounced resonator frequency fluctuations, displaying steps and periods of strong telegraphic switching as well as slow drifts.

coupled TLS of 5–7 $(\mu m^3\ GHz)^{-1}$. This is consistent with measurements of TLS densities in AlO_x tunnel junction barriers[6] when taking into account that the electric field strength in typically ≈2 nm thin barriers is about a factor of 25 larger as compared to the field strength in the capacitors employed here.

Figure 2(c) shows the absolute value of the microwave transmission $|S_{21}|$ when a coherent TLS is tuned in resonance with the resonator. The signal displays two minima whose frequencies are separated by an amount $\propto \sqrt{g^2 + (\delta/2)^2}$. By fitting these data to a model obtained with the input-output theory (see supplementary material and Ref. 16) we extract coupling strengths $g/2\pi$ between 0.5 and 1.0 MHz and TLS coherence times ranging from 102 to 363 ns. To obtain the TLS' electric dipole component $p_{\|}$ from the measured splitting size g, we estimate the electric field strength in the capacitors using SPICE simulations and find values ranging between 2.3 and 7.4 Debye (see supplementary material for individual TLS results and details on data analysis).

Spectral diffusion denotes fluctuations of the TLS' excitation energy E due to their non-resonant interaction with neighboring thermal TLS.[15] The transition energies of such thermal TLS are below $k_B\,T$ such that they experience random state switching under thermal fluctuations and therefore change the local strain and electric field. As a consequence, the detuning δ between coherent TLS and the resonator depends on time which gives rise to resonator noise induced by the fluctuating dispersive shift.[17,18] In our system, we observe pronounced frequency and phase fluctuations in the resonator due to its strong coupling to TLS in the capacitor. As an example, in Fig. 2(d), we present a series of transmission curves measured at a constant mechanical strain over a course of 35 h. One can distinguish rather quiet periods characterized by small losses and fluctuations, times with slow drifts (due to a coupling to an ensemble of thermal TLS) and also sudden steps in frequency, as well as periods with pronounced telegraphic switching between two resonance frequencies (due to a coupling to single thermal TLS).

It is well established that TLS residing on surface oxides of coplanar resonators give rise to a power dependent dielectric loss rate $\tan(\delta)$ (or the inverse internal quality factor Q_i).[19–21] Once the internal resonator power P_i exceeds a critical value P_c, the loss decreases because resonant TLS start to become saturated and act no longer as an effective photon sink.[22] The loss rate is typically modelled as

$$\tan(\delta) = Q_i^{-1} = \frac{F\tan(\delta_0)\tanh\left(\frac{\hbar\omega}{2k_BT}\right)}{\sqrt{1+(P_i/P_c)^{\beta}}} + \tan(\delta_r), \quad (1)$$

where $\tan(\delta_r)$ is a residual loss rate due to, e.g., radiative, vortex, or quasiparticle losses. $F\tan(\delta_0)$ is the dielectric loss rate of aluminum oxide dressed by a filling factor F which takes into account the participation ratio of the lossy material. Furthermore, the exponent β is introduced to account for inhomogeneous field distributions depending on the specific geometry of the device.[19,21]

In our system, we distinguish two baths of TLS: those in the surface oxide of the resonator and those in the dielectric of the overlap capacitor. We expect the latter to dominate the low-power resonator losses, because their coupling strength is orders of magnitude larger. Comparing the electric field energies in the two TLS-hosting volumes, we find participation ratios of surface and capacitor TLS $p_{surf}/p_{cap} \approx 2\text{–}9 \times 10^{-4}$, depending on the capacitor sizes.

The extracted dependence of the internal, coupling, and loaded Q-factors (Q_i, Q_C, and Q_L) on the average photon number is shown for resonator 1 in Fig. 3(a). The saturation of TLS with increasing power can be clearly seen with the increase in the internal Q-factor. A fit to Eq. (1) provides the parameters listed in Table I. The extracted critical powers P_C are for all resonators in the one-photon regime, which indicates the presence of single strongly coupled TLS. We estimate the uncertainty in the internal photon number to a factor of ≈2–3 since we had no possibility to calibrate the attenuation in the cryostat's transmission line *in-situ*.

In previous work, it has been shown that TLS produce low-frequency 1/f-phase or frequency noise in resonators,[17] and an anomalous scaling of the phase noise amplitude with temperature has been found which contradicts the predictions of the Standard Tunnelling Model.[18,23] Recently, two theories have incorporated TLS-TLS interactions in the form of spectral diffusion to explain the anomalous scaling.[24,25]

In order to test these predictions for our system, we use a homodyne detection setup depicted in Fig. 1(a). The phase noise spectral density $S_\theta(f)$ is extracted as described in Ref. 17. Figure 3(b) shows $S_\theta(f)$ for different input powers. To split the low frequency 1/f-contribution and the constant noise floor, $S_\theta(f)$ is fitted to $C(P)/f + D$, where $C(P)$ is the 1/f-noise amplitude. Its scaling with power is depicted in Fig. 3(c) for the three resonators. For our resonators, we extract the power-laws $C(P) \propto 1/P^{\beta_N}$ with $\beta_N = 0.75$, 1.00, and 0.92 which point towards a model of weakly interacting TLS[24] and agree well with previously measured data.[23]

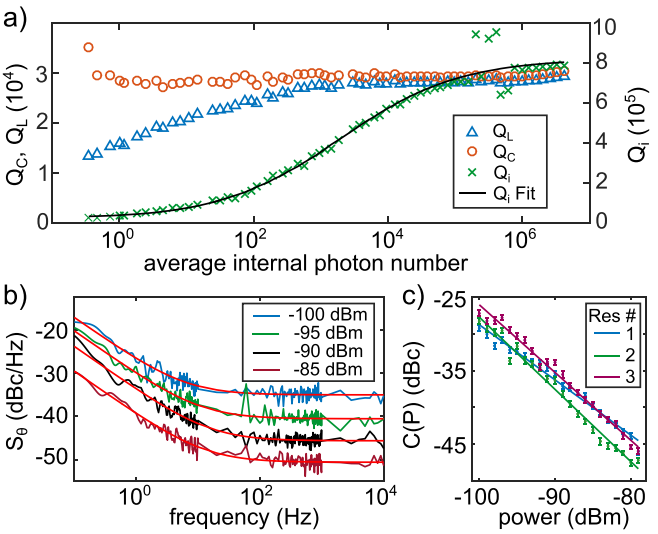

FIG. 3. (a) Power dependence of quality factors extracted from resonator 1 at 35 mK. For powers higher than the single-photon regime (> –142 dBm), the internal Q-factor Q_i increases significantly from a minimal value of 2.1 $\times 10^4$ due to TLS saturation as expected from the standard tunnelling model. A fit to Eq. (1) (solid line) results in the parameters $F\tan(\delta_0)$, P_c, and β given in Table I. (b) Power dependence of the phase noise spectral density S_θ and (c) its low frequency 1/f-noise amplitude $C(P)$.

We have presented a new method to study the properties of both single TLS and TLS ensembles by coupling an overlap capacitor with a TLS-hosting dielectric to a superconducting transmission line resonator. By applying mechanical strain to tune strongly coupled TLS near resonance with the resonator, we perform TLS spectroscopy and extract their individual dipole moments, deformation potentials, tunnel energies, and coherence times. Our system features strong coupling to a defined set of TLS and facilitates measurements of spectral diffusion and phase noise. This method can be applied to study TLS in various materials, while requiring only modest fabrication efforts and standard experimental techniques. It can become a useful tool to characterize materials employed in quantum circuits and to obtain a better understanding of the microscopic origin of TLS.

See supplementary material for additional information about individual TLS parameters and the input-output theory.

This work was funded by the Deutsche Forschungsgesellschaft (DFG), Grant No. LI2446/1-1 and partially supported by the Ministry of Education and Science of Russian Federation in the framework of Increase Competitiveness Program of the NUST MISIS (Contracts Nos. K2-2015-002 and K2-2016-063). Alexander Bilmes acknowledges support from the Helmholtz International Research School for Teratronics (HIRST) and the Landesgraduiertenförderung-Karlsruhe (LGF).

[1]W. A. Phillips, J. Low Temp. Phys. **7**, 351 (1972).
[2]P. W. Anderson, B. I. Halperin, and C. Varma, Philos. Mag. **25**, 1 (1972).
[3]P. Mohanty, D. A. Harrington, K. L. Ekinci, Y. T. Yang, M. J. Murphy, and M. L. Roukes, Phys. Rev. B **66**, 085416 (2002).
[4]R. M. J. Janssen, J. J. A. Baselmans, A. Endo, L. Ferrari, S. J. C. Yates, A. M. Baryshev, and T. M. Klapwijk, Appl. Phys. Lett. **103**, 203503 (2013).
[5]M. M. Fejer, in *Optical Interference Coatings 2016* (Optical Society of America, 2016), p. MB.1.
[6]J. M. Martinis, K. B. Cooper, R. McDermott, M. Steffen, M. Ansmann, K. D. Osborn, K. Cicak, S. Oh, D. P. Pappas, R. W. Simmonds, and C. C. Yu, Phys. Rev. Lett. **95**, 210503 (2005).
[7]K. B. Cooper, M. Steffen, R. McDermott, R. Simmonds, O. Seongshik, D. A. Hite, D. P. Pappas, and J. M. Martinis, Phys. Rev. Lett. **93**, 180401 (2004).
[8]J. Lisenfeld, C. Müller, J. H. Cole, P. Bushev, A. Lukashenko, A. Shnirman, and A. V. Ustinov, Phys. Rev. Lett. **105**, 230504 (2010).
[9]G. J. Grabovskij, T. Peichl, J. Lisenfeld, G. Weiss, and A. V. Ustinov, Science **338**, 232 (2012).
[10]J. Lisenfeld, G. Grabovskij, C. Müller, J. Cole, G. Weiss, and A. Ustinov, Nat. Commun. **6**, 6182 (2015).
[11]J. Lisenfeld, A. Bilmes, S. Matityahu, S. Zanker, M. Marthaler, M. Schechter, G. Schön, A. Shnirman, G. Weiss, and A. V. Ustinov, Sci. Rep. **6**, 23786 (2016).
[12]A. Bilmes, S. Zanker, A. Heimes, M. Marthaler, G. Schön, G. Weiss, A. V. Ustinov, and J. Lisenfeld, Phys. Rev. B **96**, 064504 (2017).
[13]B. Sarabi, A. N. Ramanayaka, A. L. Burin, F. C. Wellstood, and K. D. Osborn, Phys. Rev. Lett. **116**, 167002 (2016).
[14]A. Blais, R.-S. Huang, A. Wallraff, S. M. Girvin, and R. J. Schoelkopf, Phys. Rev. A **69**, 062320 (2004).
[15]W. A. Phillips, Rep. Prog. Phys. **50**, 1657 (1987).
[16]B. Sarabi, A. N. Ramanayaka, A. L. Burin, F. C. Wellstood, and K. D. Osborn, Appl. Phys. Lett. **106**, 172601 (2015).
[17]J. Gao, J. Zmuidzinas, B. Mazin, H. LeDuc, and P. K. Day, Appl. Phys. Lett. **90**, 102507 (2007).
[18]J. Burnett, L. Faoro, I. Wisby, V. Gurtovoi, A. V. Chernykh, G. Mikhailov, V. Tulin, R. Shaikhaidarov, V. Antonov, P. Meeson, A. Y. Tzalenchuk, and T. Lindström, Nat. Commun. **5**, 4119 (2014).
[19]J. M. Sage, V. Bolkhovsky, W. D. Oliver, B. Turek, and P. B. Welander, J. Appl. Phys. **109**, 063915 (2011).
[20]H. Wang, M. Hofheinz, J. Wenner, M. Ansmann, R. C. Bialczak, M. Lenander, E. Lucero, M. Neeley, A. D. O'Connell, D. Sank, M. Weides, A. N. Cleland, and J. M. Martinis, Appl. Phys. Lett. **95**, 233508 (2009).
[21]J. Goetz, F. Deppe, M. Haeberlein, F. Wulschner, C. W. Zollitsch, S. Meier, M. Fischer, P. Eder, E. Xie, K. G. Fedorov, E. P. Menzel, A. Marx, and R. Gross, J. Appl. Phys. **119**, 015304 (2016).
[22]M. V. Schickfus and S. Hunklinger, Phys. Lett. A **64**, 144 (1977).
[23]A. N. Ramanayaka, B. Sarabi, and K. D. Osborn, preprint arXiv:1507.06043 (2015).
[24]A. L. Burin, S. Matityahu, and M. Schechter, Phys. Rev. B **92**, 174201 (2015).
[25]L. Faoro and L. B. Ioffe, Phys. Rev. B **91**, 014201 (2015).